Available online at www.sciencedirect.com
ScienceDirect
Trans. Nonferrous Met. Soc. China 27(2017) 1294−1305
Transactions of Nonferrous Metals Society of China
www.tnmsc.cn

Morphology transformation of primary strip α phase in hot working of two-phase titanium alloy

Xiao-guang FAN, He YANG, Peng-fei GAO, Rui ZUO, Peng-hui LEI, Zhe JI

State Key Laboratory of Solidification Processing, School of Materials Science and Engineering, Northwestern Polytechnical University, Xi'an 710072, China

Received 4 March 2016; accepted 30 September 2016

Abstract: Microstructural development in hot working of TA15 titanium alloy with primary strip α structure was investigated with the aim to globularize α strips. Results show that the mechanisms of morphology transformation are the same to the spheroidization mechanisms of lamellar structure. Boundary splitting and termination migration are more important than coarsening due to the large size of strip α. The α strips are stable in annealing due to the unfavorable geometrical orientation of intra-α boundaries, the large thickness of strip and the geometrical stability of α particles. Predeformation and low speed deformation accelerate globularization of α strips in the following ways: direct changing of particle shape, promotion of boundary splitting and termination migration by increasing high angle grain boundaries and interfacial area, promotion of coarsening by forming dislocation structures. Large predeformation combined with high temperature annealing is a feasible way to globularize strip α.
Key words: titanium alloy; primary α strips; globularization; morphology transformation; hot working; coarsening

1 Introduction

Titanium alloys have gained increasing applications due to the high specific strength and good corrosion resistance. Hot working is often employed to transform the lamellar structure to equiaxed structure, so the ductility and fatigue resistance can be improved. This is commonly referred to globularization or spheroidization. Globularization of lamellar structure occurs during primary working, in which ingots are transformed to semi-products by rotary forging or rolling [1]. The large unidirectional elongation of work-piece will affect the morphology of α phase. Some α phases may appear in strip form with high aspect ratio (they are referred to as strip α herein and after) under improper processing route. To enhance the isotropy and fatigue resistance of material, the strip α should be transformed to globular ones.

By now, most work on the morphology transformation of α phase was about the globularization of lamellar α. It begins with the loss of coherency of α/β interfaces [2] and formation of boundaries across α platelets by deformation [3]. The intra-α boundaries can be subgrain boundaries produced by dynamic recovery or high angle boundaries caused by dynamic recrystallization [4,5]. The intra-α boundary creates unstable dihedral angle with neighboring α/β interface. To lessen surface tension, β phase wedges into α platelets along the boundary so that the dihedral angle is reduced and stabilized [6]. The so called thermal grooving splits α platelets into particles with lower aspect ratio. α lamellae can be further globularized by termination migration and Ostwald ripening [6]. The first stage of globularization is deformation induced. Meanwhile, the second and third stages are diffusion controlled and time dependent. So globularization occurs dynamically during deformation and statically in the subsequent heat treatment.

Globularization kinetics is sensitive to processing parameters. Dynamically globularized fraction increases with strain in a sigmoidal way [7]. A critical strain is required for the initiation. The globularization rate increases with increasing temperature and decreasing strain rate. On the other hand, the statically globularized fraction increases with the increase of time in an

Foundation item: Projects (51205317, 51575449) supported by the National Natural Science Foundation of China; Project (3102015AX004) supported by the Fundamental Research Funds for the Central Universities, China; Project (104-QP-2014) supported by the Research Fund of the State Key Laboratory of Solidification Processing, China
Corresponding author: Xiao-guang FAN; Tel: +86-29-88460212; E-mail: fxg3200@nwpu.edu.cn
DOI: 10.1016/S1003-6326(17)60150-X

asymptotic way [8,9]. It increases with applied strain and holding temperature but is less sensitive to strain rate.

Break-down of strip α may be similar to globularization of lamellar α. However, a previous work [10] suggested that break-down of α strips was so sluggish that globularized structure was not observed at 80% reduction. This might be caused by the lack of second and third stages, i.e., α strips may have already broken into several grains but were not separated by β phase. As the width of α strips is much larger than that of α lamellae, the required time for static globularization is much longer.

The morphology transformation can be speeded up if the diffusion of solutes is accelerated, as both the second and third stages are diffusion controlled. This can be achieved by imposing low speed deformation at high temperature. SEMIATIN et al [11] reported that dynamic coarsening rates were enhanced by 5 times relative to those for static coarsening. Also, it has been reported in many alloys that fiber structure becomes globular after superplastic deformation, which also occurs at a low strain rate. The titanium alloy exhibits excellent superplasticity. MOTYKA et al [12] have reported spheroidization of predeformed lamellar α of Ti−6Al−4V alloy during superplastic deformation. The α strips may be broken down in the same way.

In this work, different hot working schemes were used to globularize strip α phase produced in rolling. The morphology transformation was quantitatively measured. Feasible processing route for globularization of strip α was proposed. The results can be used to improve the microstructure of titanium alloy products.

2 Experimental

A near-α TA15 titanium alloy was employed in this work. The as-received material was an 18 mm-diameter hot rolled bar with measured chemical composition of Ti−6.06Al−1.86Zr−2.08Mo−1.32V (mass fraction, %) and β-transus temperature was 985 °C. The initial structure consisted of about 50% primary α within transformed β matrix, as shown in Fig. 1. The primary α particles were elongated in the rolling direction. Meanwhile, they had irregular cross sections. So, the α particles were rod-like with the axis parallel to the rolling direction. Herein and after, the α particle denotes the α phase isolated by β matrix. A α particle may contain several α grains which cannot be differentiated by the optical micrograph or SEM [13]. This was confirmed by electron backscatter diffraction (EBSD) analysis (Fig. 2). The crystal orientation varied in the α particle. There existed boundaries inside α strips (black lines in Fig. 2).

Three working schemes were used to globularize strip α. The material was annealed at 930 and 970 °C for 0.5−16 h. The material was deformed at 930 °C to 40% reduction at strain rate of 0.1 s^{-1} and then annealed at 970 °C for 0.5−16 h. The material was deformed at temperatures of 930 and 970 °C, strain rates of 1×10^{-3} and 1×10^{-4} s^{-1} to true strains of 0.6, 1.2 and 1.8.

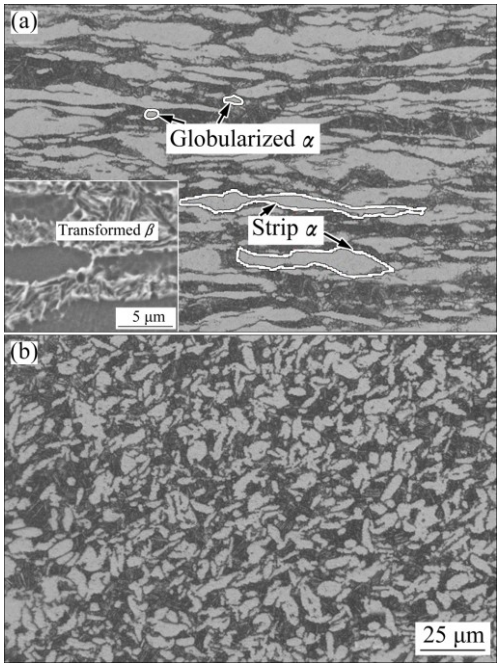

Fig. 1 Optical micrograph of as received hot rolled bar: (a) Axial section; (b) Cross section (The axial direction (rolling direction) is horizontal in Fig. 1(a))

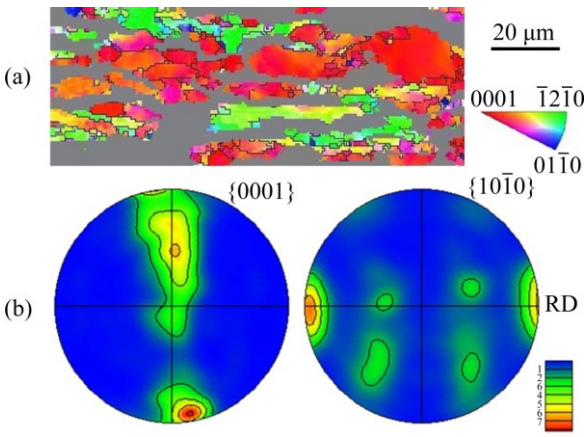

Fig. 2 Inverse pole figure map (a) and pole figures (b) of strip α

High temperature deformation was conducted on a SANS CMT5205 electric universal testing machine. The specimens were cylinders of 15 mm in diameter and 24 mm in height with the axis parallel to rolling direction. They were heated to the deformation temperature at 12 °C/min, held for 15 min and compressed. The constant anvil speed was used throughout deformation. Here, the die speed was set to be 1.5×10^{-2} and 1.5×10^{-3} mm/s so that the average strain rate for different height reductions was close to the set value.

All the specimens were air cooled after hot working. Secondary α would precipitate from β matrix during cooling. The transformed β matrix was easily distinguished from primary α, which facilitated the identification of α−β interfaces. Meanwhile, the cooling rate was high enough to suppress the diffusional growth of primary α.

Microstructure was observed on axial and equatorial planes of the specimen, which corresponded to the axial and cross sections of the rolled bar. The morphology of α particle was characterized by its aspect ratio. It was measured with micrographs taken on the axial section. The α particle was rod-like with its major axis parallel to compression axis, and the measured aspect ratio would be close to its length-to-diameter ratio. A α particle with aspect ratio above 2.5 was taken as strip α. The lineal-path correlation function and two-point correlation function were used to characterize the spatial arrangement of α particles [14]. The lineal-path correlation function $L_{11}(r, \theta)$ is defined as the probability that a segment with length of r and orientation of θ is in a single α particle. The two-point correlation function $P_{11}(r, \theta)$ is the possibility that a segment with length of r and orientation of θ begins and finishes in the α phase. $P_{11}(r, \theta)$ fulfills the following constraint:

$$\lim_{r\to\infty} P_{11}(r,\theta)=f_1^2 \quad (1)$$

where f_1 is the volume fraction of α phase. Therefore, the normalized correlation function $P_{11}(r,\theta)/f_1^2$ was adopted. θ was calculated relative to the major axis of the α strip, i.e., 0°, when the segment was parallel to the α strip.

3 Results and discussion

3.1 Microstructure evolution during heat treatment

In hot working, the phase transformation during heating and cooling may affect the microstructure significantly. α to β transformation occurs during heating. For an isolated α particle, the dissolution rate is inversely proportional to its radius. So, the small particles with low aspect ratio were prone to dissolution while the large strip α with less curved α−β interfaces was left, as shown in Fig. 3(a). The width of the strip α varied sharply on the axial section as some of them had lathy cross section (left bottom of Fig. 3(a)). They showed large width when the section plane was parallel to their broad faces.

During cooling, the volume fraction of primary α phases increases at a low cooling rate due to the epitaxial growth of α particles. Both the length and width of α strips are increased. The morphology changes little after cooling. So, the effect of cooling is ignored in this work.

The morphology of α strips varied little after annealing at 930 °C for 1 h (Fig. 3(b)). But the grooves were more clearly observed on the strips, as indicated by the red arrows in Fig. 3(b). This was because the kinetics of boundary splitting was much higher than that of Ostwald ripening and termination migration. PARK et al [6] and STEFANSSON et al [15] reported that the time required for boundary splitting was about 1 h in two-phase region while the completion of termination migration required tens of hours. Due to the morphology of the strip, grooves were more clearly observed on axial section.

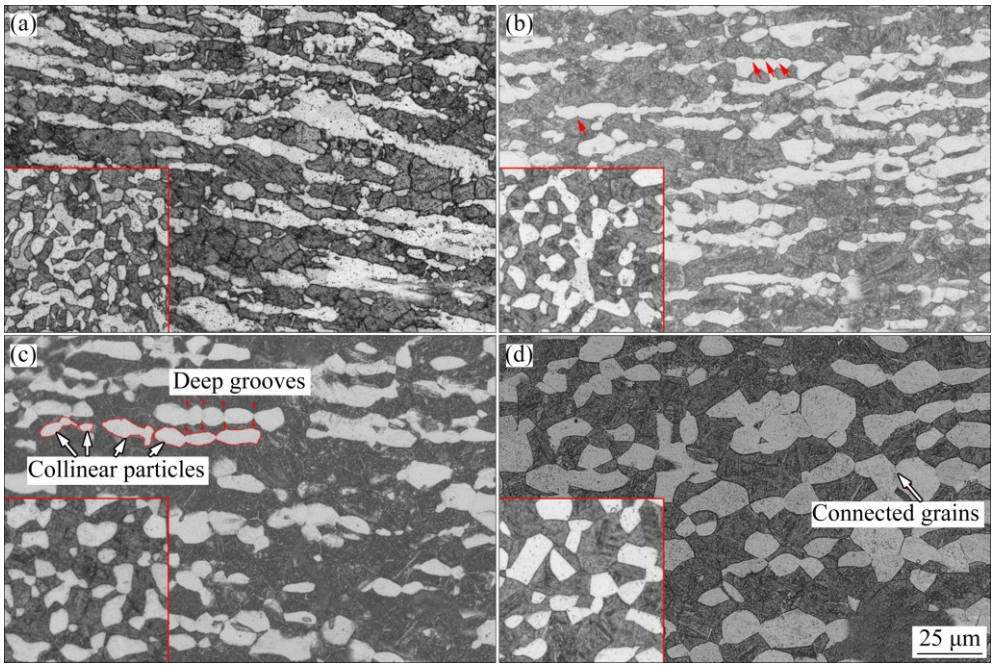

Fig. 3 Microstructures developed after annealing at 930 °C for 15 min (a), 1 h (b), 4 h (c) and 16 h (d) (Microstructure on cross section is shown on left bottom)

Coarsening was significant after annealing for 4 h, as shown in Fig. 3(c). The strip thickness on axial section and the particle size on cross section increased while the number of α particles dropped dramatically. On the other hand, the density of the intra-α boundaries was greatly reduced. EBSD measurement showed that the α−α boundaries became straight and perpendicular to the strips (Fig. 4). Moreover, 75% of the intra-α boundaries were high angle grain boundaries (>15°). This promoted the splitting of strip α. They were further broken into several collinear α particles. Pairs of deep grooves were also observed on the remnant short strips, resulting in a necklace structure of α grains (Fig. 3(c)). Cross section of strip α became more equiaxed, which could also be interpreted in terms of thermal grooving and termination migration.

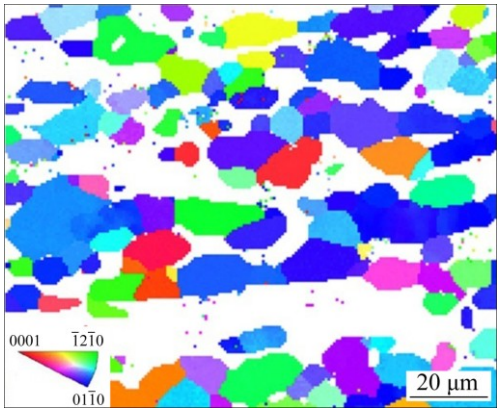

Fig. 4 Inverse pole figure map for specimen annealed at 930 °C for 4 h

On both axial and cross sections, the α−β interfaces at the grooves become flat. The angle between the two interfaces was about 120°. The α−α grain boundary energy is similar to the α−β interfacial energy (about 0.4 J/m^2) [16]. A steady triangle boundary structure had already formed. Boundary splitting, which was driven by the stabilizing of dihedral angle, finished after 4 h holding.

With increasing holding time, α particles were further coarsened, as shown in Fig. 3(d). However, some short α strips still existed. Taking the vertexes at the grooves as the locations of intra-α boundaries (this has been validated by Fig. 4), the α strip consisted of grains with low aspect ratio. Meanwhile, the particle size on the cross section was close to the groove interval. It might be deduced that α grains were nearly spherical in shape. As a result, termination migration was negligible. Further break-down of the connected α grains would be achieved only by Ostwald ripening.

The microstructure evolution at a high annealing temperature is shown in Fig. 5 (The micrographs on cross section were not presented hereafter as they were similar to those presented in Fig. 3). More α phases were transformed at higher annealing temperatures. Some of the α strips were broken down due to phase transformation at the grooves. So, the average aspect ratio decreased slightly. However, long α strips still took a large fraction. Thermal grooving played a more important role under short annealing time (Fig. 5(a)). STEFANSSON et al [15] found that the boundary splitting time for static globularization of Ti−6Al−4V was reduced from 10 to 1 h when the annealing temperature increased from 900 to 955 °C. Though the high temperature promoted thermal grooving and termination migration, strings of connected α grains still existed after prolonged annealing (Fig. 5(b)). Thus, α strips are more stable than wrought α lamellae.

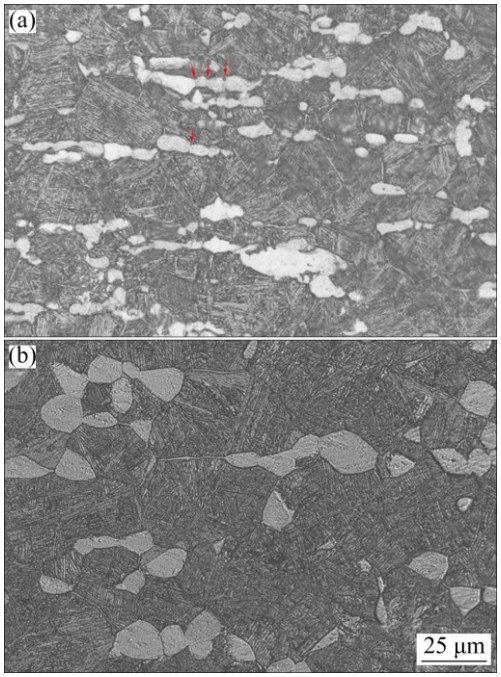

Fig. 5 Microstructures developed after annealing at 970 °C for 0.5 h (a) and 16 h (b)

The measured average aspect ratio and globularized fraction are given in Fig. 6. Annealed at a relatively low temperature (930 °C), the average aspect ratio and globularized fraction varied slightly in the early stage (The fluctuation might be caused by the error of measurement). Then, it decreased sharply with time. On the other hand, a rapid decrease in aspect ratio occurred at 970 °C in the first 2 h. The globularized fraction also increased sharply. This confirms that high annealing temperature can greatly accelerate the boundary splitting.

It is interesting to notice that the globularized fraction increased little during prolonged annealing and it became close irrespective of temperature. So did the average value and distribution of aspect ratio. Though average aspect ratio was less than 3, the globularized

fraction was below 50%. This suggests that globularization by termination migration and coarsening is very limited in current study. The break-down of α strips mainly depends on the structure of α strips, i.e., the length and width of α strips as well as the intra-α boundaries. These factors determine the boundary splitting process. So, it is hard to obtain a fully globularized structure by annealing. One reason that limits the globularization during prolonged annealing may be the geometry of α particles. α strips were straight, which had relatively low surface area, so, they were stable during coarsening.

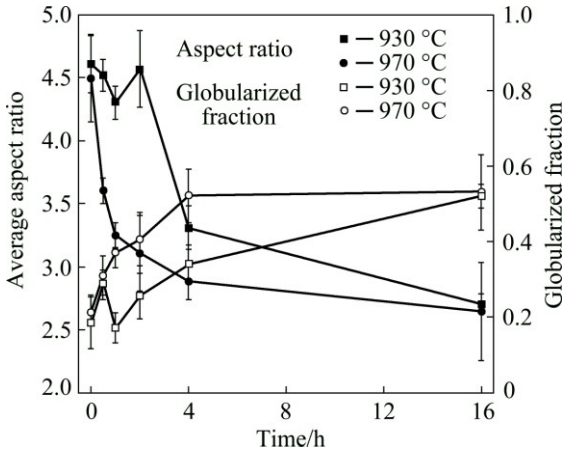

Fig. 6 Variation of average aspect ratio and globularized fraction during annealing

The spatial distribution of α particles was characterized by the lineal-path correlation function and two-point correlation function, as shown in Fig. 7. As the lineal-path correlation function approaches the volume fraction of α phases when r approaches 0, all the curves are normalized according to the average α fraction.

After annealing at 930 °C, the lineal-path correlation function along the major axis of the α strips varied little with time. This meant that the particle size along this direction did not change. A similar behavior was also observed in the two-point correlation function (Fig. 7(b)). Thus, the distribution of α particles varied little.

The lineal-path correlation function along the minor axis dropped more slowly with longer holding time, indicating significant increase in particle size along this direction. The variation of two-point correlation function was similar (Fig. 7(b)), in which the decreasing rate was also related to the particle size. The two-point correlation function reaches the steady state when the r is about the average particle size. The particle size along the minor axis increased by once after 16 h annealing. The difference between the two directions diminished due to coarsening.

After annealing at 970 °C, the variation of lineal-path correlation function along the minor axis was similar to that at 930 °C. The change along the major axis was more significant. The lineal-path correlation function dropped more quickly after annealing, indicating the break-down of α strips. But the discrepancy still existed after 16 h annealing.

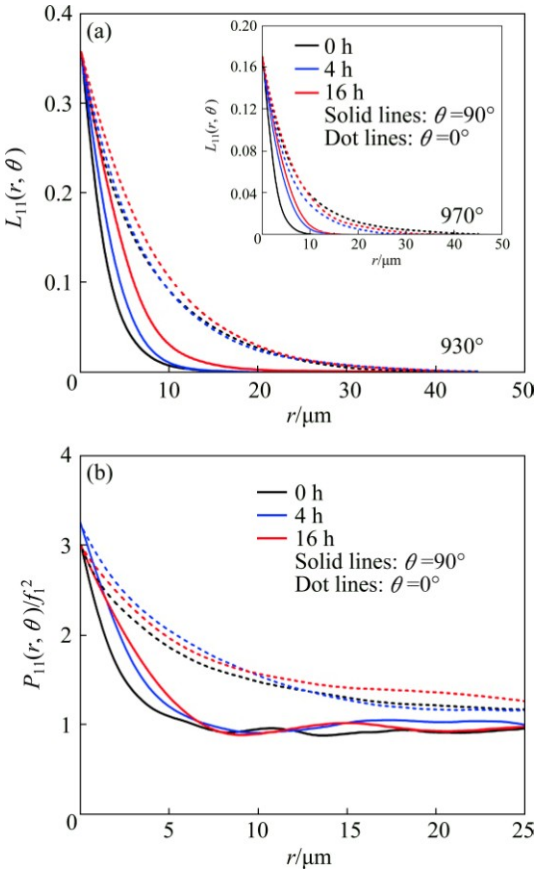

Fig. 7 Variation of lineal-path correlation function (a) and two-point correlation function (b) during annealing

Globularization of strip α during annealing is similar to static globularization of lamellar α. It is also determined by three key factors: boundaries inside α strips, splitting of α strips and coarsening of α particles. As the work-piece had undergone large deformation, there were plenty of α−α boundaries (Fig. 2). So, boundary splitting and coarsening were important to morphology transformation. Unlike the static globularization of lamellar structure, the globularization of strip α was limited. The stability of strip α may be attributed to the following factors.

1) Geometrical orientation of the intra-α boundaries was unfavorable. A lot of boundaries randomly distributed in α strips (Fig. 2). They gradually became perpendicular to α strips and served as penetration routes of β phase. This process was time consuming. Moreover, lots of intra-α boundaries have been annihilated (Figs. 2 and 4).

2) The α strips were thick. STEFANSSON and SEMIATIN [15] estimated the time for boundary

splitting by the following equation:

$$t=\left(\frac{Y_0}{0.86mA}\right)^n \tag{2}$$

where Y_0 is the half thickness of the strip, m is the slope of the penetrating boundary, A is a constant and n is the coarsening exponent. n is about 3, as the coarsening process is controlled by bulk diffusion (this will be discussed in section 3.4). So, the time for boundary splitting increases cubically with the thickness of α strip. Meanwhile, the coarsening can further retard boundary splitting. So, a lot of grooved strips existed after prolonged annealing (Fig. 3(d)).

3) The geometry of the particles retarded the termination migration. The straight α strips had relatively low interfacial area. They were stable during coarsening.

3.2 Effect of predeformation

The globularization kinetics was greatly affected by predeformation, as shown in Fig. 8. The average aspect ratio reduced after predeformation. Then, it decreased slightly during annealing. The variation of aspect ratio after 1 h annealing was almost the same to that of undeformed material. So did the globularized fraction.

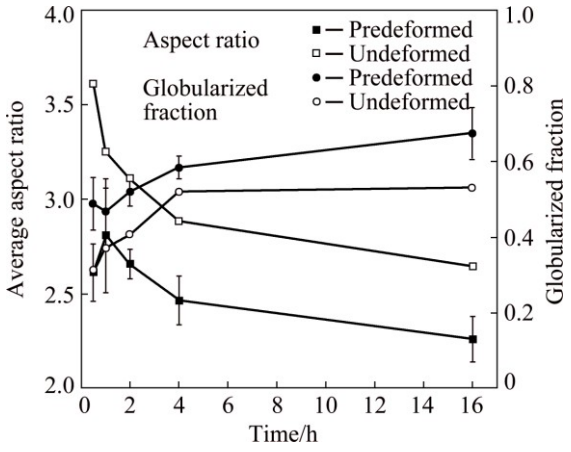

Fig. 8 Effect of predeformation on globularization kinetics

The microstructure of deformed specimen is given in Fig. 9. The microstructural change was trivial after deformation. So, α strips were not globularized dynamically by deformation. However, some of the α strips were kinked. The primary α phase is 3−4 times the strength of β matrix [17]. Moreover, the as-received material exhibited a strong $\{10\bar{1}0\}_\alpha$ phase partial fiber texture with fiber axis parallel to the rolling direction, as shown in Fig. 2. The fiber texture is often produced in extrusion, but also reported for cogging and radial forging which have a similar strain path [13]. As the c-axis of most grains was perpendicular to the rolling direction, it was also perpendicular to compression axis. Easy slip was only possible on prism planes [18]. The α phase was in hard orientation. This resulted in heterogeneous deformation in the material and the α strips were prone to kinking. This phenomenon has been reported in the globularization of lamellar structure [18,19].

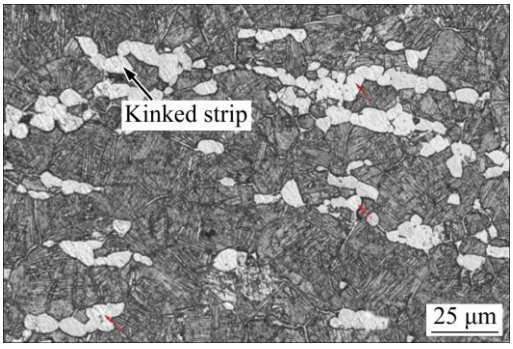

Fig. 9 Microstructure developed after deformation at 930 °C and annealing at 970 °C for 0.5 h

The decrease in aspect ratio was caused by the kinking of α strips. Apparently, the kinked α strips had low aspect ratio. Moreover, the kinked strips had more terminals (kinks served as terminals) and larger surface area. They were more likely to evolve to isolated grains by termination migration. That accounted for the fact that more α strips were globularized after 4 h annealing. Also, strain concentration occurred in the kinked areas. The crystal defects promoted the splitting at the kinks. This has been reported for the globularization of lamellar α of titanium alloy [20].

Kinking resulted in more randomly distributed α particles. The discrepancy between the correlation functions along different directions decreased (Fig. 10). $L_{11}(r, 0)$ approached 0 more rapidly with r after predeformation (Fig. 10(a)). Thus, the residual long α strips were reduced. The two-point correlation function varied little with annealing time, suggesting that the distribution of α particles was not changed during annealing (Fig. 10 (b)).

3.3 Effect of low speed deformation

Typical microstructures after low speed deformation are shown in Fig. 11. The α−β interface was relatively smooth at temperature of 930 °C and strain rate of 1×10^{-4} s^{-1} (Fig. 11(b)). Meanwhile, α strips were kinked but less pancaked. By contrast, α strips were pancaked and α−β interfaces were curved under other deformation conditions. It may be deduced that superplastic deformation occurred at 930 °C and strain rate of 1×10^{-4} s^{-1} while dislocation activity was the main deformation mechanism for other deformation conditions in this work.

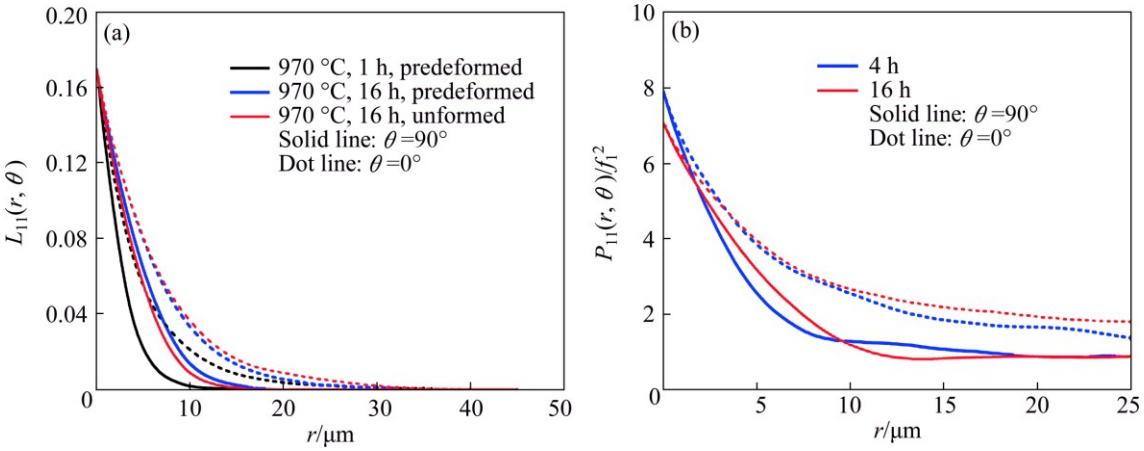

Fig. 10 Measured lineal-path correlation functions (a) and two-point correlation functions (b) of predeformed material

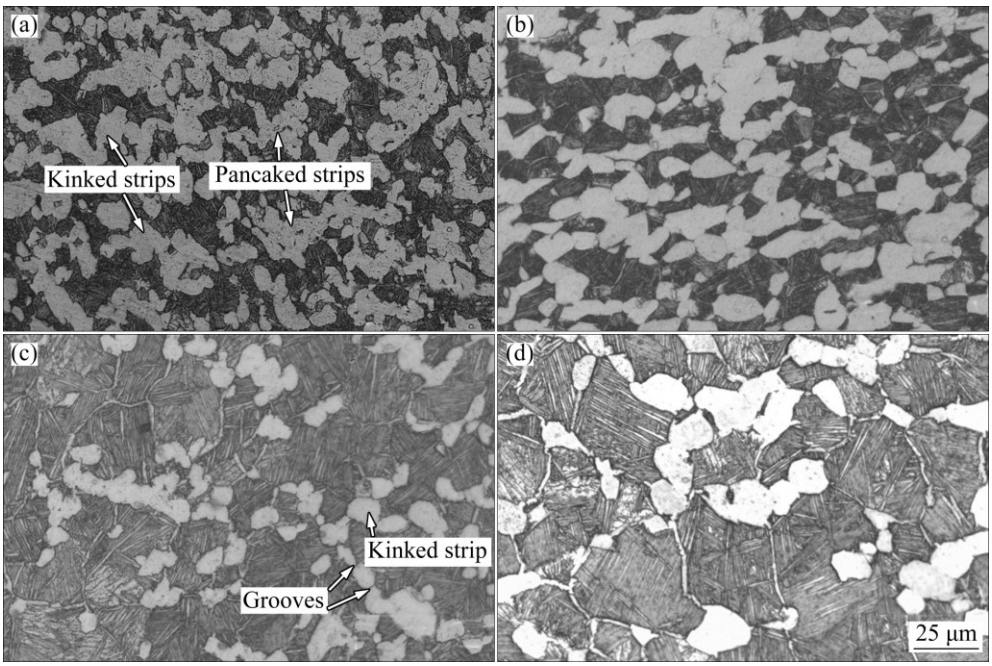

Fig. 11 Microstructures developed after low speed deformation to strain of 1.2: (a) 930 °C, 1×10^{-3} s^{-1}; (b) 930 °C, 1×10^{-4} s^{-1}; (c) 970 °C, 1×10^{-3} s^{-1}; (d) 970 °C, 1×10^{-4} s^{-1}

The strain rate sensitivity (m value) was obtained by isothermal compression tests (including strain rate jump tests and constant strain rate compressions), as shown in Fig. 12. Strain rate jump tests and constant strain rate compressions gave similar results at low strain rates (1×10^{-4} s^{-1}–1×10^{-3} s^{-1}). The value of m was as high as 0.75 at 930 °C and 1×10^{-4} s^{-1}, indicating the occurrence of superplastic deformation [21]. It decreased sharply with strain rate. m was about 0.35 at 1×10^{-3} s^{-1} and 0.2 at 1×10^{-2} s^{-1} with the strain rate jump test. The governing mechanism may be power law creep or dislocation glide [11]. Strain rate sensitivity decreased with strain increasing at strain rate of 1×10^{-4} s^{-1}, which might be attributed to the decrease of boundaries due to coarsening. So, dislocation activity accounted for larger fraction of deformation with increasing strain. At 970 °C,

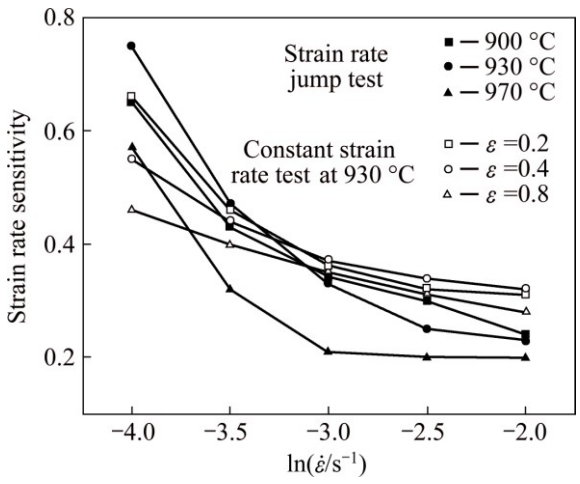

Fig. 12 Strain rate sensitivity determined from strain rate jump test and constant strain rate compression

the values of m were about 0.58 and 0.2 at strain rates of 1×10^{-4} s^{-1} and 1×10^{-3} s^{-1}. Strain rate sensitivity was typical for superplastic deformation at 1×10^{-4} s^{-1}. However, due to the rapid coarsening, more strain was accommodated by dislocation movements. As a result, pancaked α particles with curved boundaries were observed (Fig. 11(d)).

The processing window for superplasticity was narrow in this work. A lot of work reported superplastic deformation at strain rate of 1×10^{-3} s^{-1} for two-phase titanium that alloy. For instance, SEMIATIN et al [11] estimated that only 1% of the deformation was accommodated by dislocation glide/climb for ultrafine-grained Ti−6Al−4V alloy deformed at 900 °C and 1×10^{-3} s^{-1} while the other via grain boundary sliding. Apparently, this is not the case in this work. This is because the larger grain size and elongated grain morphology prohibited the boundary sliding.

In the absence of superplastic deformation, the compressive deformation along the major axis of α strips was important for morphology change especially at low temperature and high strain rate. At 930 °C and 1×10^{-3} s^{-1}, α strips were pancaked or severely kinked (Fig. 11(a)). Grooves were very limited on the strips. The morphology change was attributed to the deformation of α strips. The aspect ratio decreased with strain and then increased (Fig. 13). The globularized fraction also decreased after critical strain, as the α particles were elongated perpendicular to the compression axis. Though the faction of low aspect ratio α was over 80% at proper strain, some of the α strips were kinked and compressed instead of globularized.

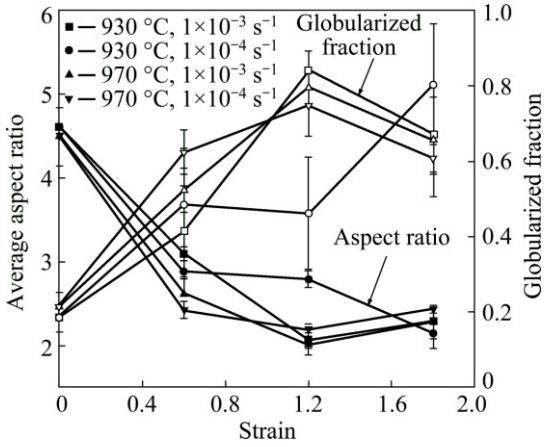

Fig. 13 Variation of aspect ratio and globularized fraction during low speed deformation

With increasing deformation temperature (970 °C, 1×10^{-3} s^{-1}), α particles were less deformed as the strain partitioning between α and β phases increased with decreasing α content. So, α strips were kinked but less upset (Fig. 11(c)). Meanwhile, the deformation in β matrix promoted thermal grooving due to the pipe diffusion through crystal defects. There were deep thermal grooves and observable boundaries inside the kinked particles, indicating the acceleration in globularization of α strips. So, both deformation and thermal grooving affect the microstructure morphology. As deformation induced morphology change was weakened, the variation in aspect ratio was smaller (Fig. 13).

With decreasing strain rate, thermal grooving, termination migration and coarsening played more important roles. The globularized fraction was over 60% at a strain of 0.6, 970 °C and strain rate of 1×10^{-4} s^{-1} (Fig. 13). Meanwhile, thickening of α strips was more significant. As a result, strip kinking was not obvious (Fig. 11(d)). The microstructure becomes stable. The average aspect ratio varies little with strain.

The lineal-correlation functions along both directions were changed by imposing strain. The difference between the two correlation functions decreased with strain and then increased (Fig. 14), which was similar to the evolution of aspect ratio. So did the two-point correction function (Fig. 15). Both the spatial

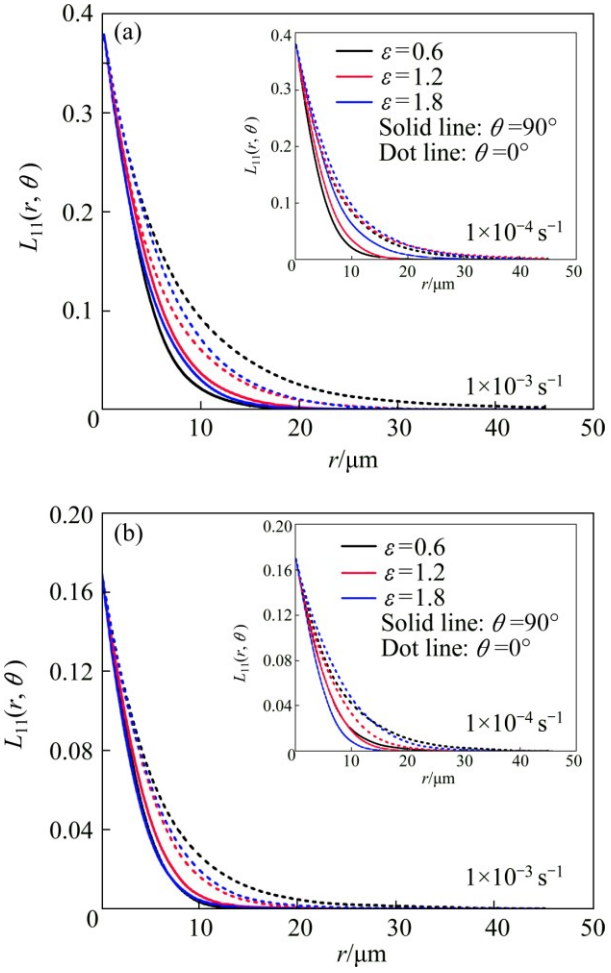

Fig. 14 Variation of lineal-path correlation function during low speed deformation: (a) 930 °C; (b) 970 °C

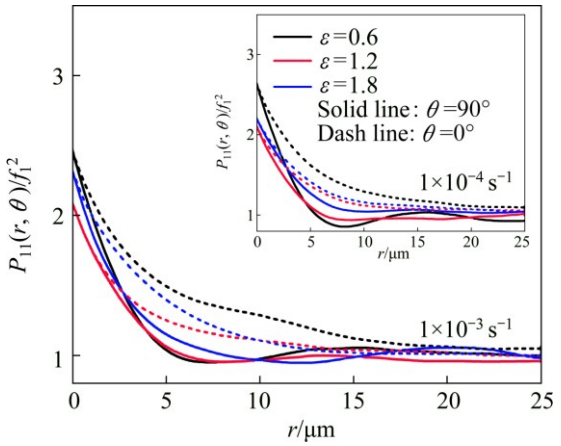

Fig. 15 Variation of two point correlation function during low speed deformation at 930 °C

distribution and morphology of α strips were changed by deformation. The variation of the lineal-path correlation function with strain was more significant at a low strain rate due to additional coarsening (Fig. 14 (a)).

In superplastic deformation, α strips became kinked instead of pancaked (Fig. 11(b)). Most of the strain was accommodated by boundary sliding. Both α−β interfaces and α−α grain boundaries were involved in superplastic deformation. Rotation of α phase resulted in kinked and random aligned α particles and promoted boundary splitting and termination migration. Meanwhile, coarsening was significant as the deformation time was long. As a result, the aspect ratio decreased monotonically with strain (The measured average aspect ratio scattered because some kinked strips contacted each other). Superplastic deformation also changed the spatial distribution of α phase. The difference between correlation functions along different directions was greatly reduced with strain (Figs. 14 and 15). The two-point correlation functions almost coincided at strain of 1.8. Moreover, the rotation of α phase weakened the texture, as shown in Fig. 16. The strong $\{10\bar{1}0\}_\alpha$ phase partial fiber texture was weakened with strain increasing. So, the microstructure becomes more isotropic after superplastic deformation.

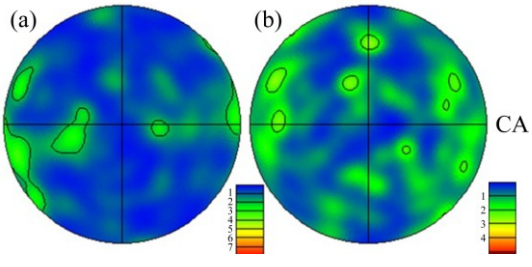

Fig. 16 Pole figures of α phase $\{10\bar{1}0\}$ after deformation at 930 °C and strain rate of 1×10^{-4} s^{-1} to strains of 0.6 (a) and 1.2 (b)

Both predeformation and low speed deformation can promote the globularization of strip α. The roles of deformation in morphology transformation are as follows: 1) Deformation and kinking of α strips directly change the morphology; 2) The increased high angle grain boundaries and interfacial area due to strip kinking promote boundary splitting and termination migration; 3) The dislocation structures promote coarsening induced globularization. Kinking of α strips greatly accelerates the globularization process. So, deformation is important to the break-down of long α strips. Moreover, deformation also improves the spatial distribution of α particles.

3.4 Coarsening during hot working

In annealing and low speed deformation, coarsening is inevitable and it is also one of the most important mechanisms of morphology transformation. Coarsening may weaken the performance of work-piece. Therefore, it is evaluated in this work. Coarsening of secondary phases is known as Ostwald ripening. The Lifshitz−Slyozov−Wagner (LSW) theory was used to quantify this phenomenon. The evolution of particle size fulfilled the following equation [22]:

$$r^n - r_0^n = K(t - t_0) \tag{3}$$

where r is the average particle radius, r_0 is the initial value at t_0, and K is the coarsening rate constant. The coarsening exponent n is 3 for bulk diffusion control and 4 for grain boundary diffusion control.

The classical LSW theory is developed for the coarsening problem involving small fraction of spherical particles. It may not be suitable for this work because the α strips were rod-like. A α strip was composed of several α grains with low aspect ratio (Figs. 2 and 4). These grains gradually became isolated during annealing. The section size of the strip α might be a proper parameter to quantify coarsening, as it was close to the size of the constituent grains. It was found that the measured particle size distributions were essentially self-similar. The average particle size measured from the cross section was used to estimate the coarsening behavior.

The measured particle size is shown in Fig. 17. As expected, coarsening was sluggish in annealing. But it was greatly promoted by low speed deformation. Predeformation did not affect the grain growth. The crystal defects by predeformation could promote the diffusion of solutes. The Ostwald ripening, which is commonly governed by bulk diffusion through the β matrix, should be speeded up. However, the annihilation of crystal defects was fast at high temperature while the diffusion controlled microstructure development was sluggish. So, the microstructure coarsening was less affected by predeformation.

The coarsening exponent was determined to be 4−5 by fitting to the experimental data, as shown in Table 1. On the other hand, WU et al [23] found that n was about 3 at 940 and 970 °C for the same material. The deviation might be caused by the relatively short annealing time in this work. A small fluctuation in the measured particle size would result in great change in coarsening exponent because grain growth is slow for two-phase titanium alloy. The annealing time was as long as 60 h. So, the result is more reliable. SEMIATIN et al [24] also reported a coarsening exponent of about 3 for two-phase Ti−6Al−4V alloy. So did the near β Ti17 alloy [25].

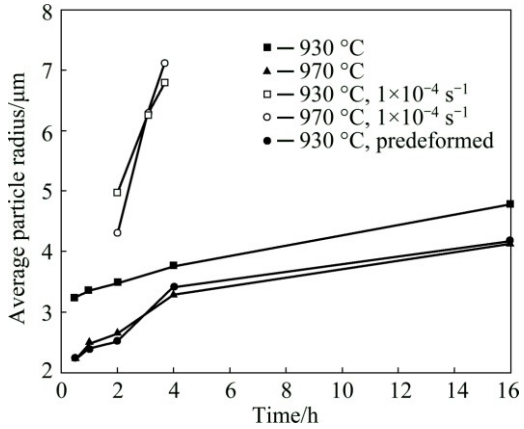

Fig. 17 Measured average particle size after hot working

Table 1 Coarsening exponents under different hot working conditions

930 °C	970 °C	970 °C, predeformed	930 °C, 1×10^{-4} s^{-1}	970° C, 1×10^{-4} s^{-1}
4.2	4.8	4.5	3.1	2.2

Coarsening exponent was 2−3 under low speed deformation. Though the result indicated a behavior controlled by bulk diffusion and interface migration, SEMIATIN et al [11] suggested that it was also governed by bulk diffusion.

Assuming the same coarsening exponent of 3, the coarsening rate constant was enhanced by 15 times when low speed deformation was imposed, as shown in Table 2. It is higher than that reported by STEFANSSON and SEMIATIN [15] (about 5 times). Static coarsening rate (annealing), however, is close to that in their work (5−7 $\mu m^3/h$). SEMIATIN et al [13] suggested that superplastic deformation suppressed the dislocation activity. So, the coarsening rate was less than that expected. In this work, dislocation activity played a more important role in deformation. This might accelerate the diffusion of solutes in hot working.

Table 2 Coarsening rates under different hot working conditions ($\mu m^3/h$)

930 °C	970 °C	970 °C, predeformed	930 °C, 1×10^{-4} s^{-1}	970 °C, 1×10^{-4} s^{-1}
5.90	4.64	4.50	73.2	81.9

3.5 Method of microstructure modification

Two particulars should be done to globularize α strips: decreasing the stability of the strips and promoting the splitting of strips. Both of them can be achieved by low speed deformation. However, as they occur simultaneously, it may need a long time (or a large strain). For instance, the globularized fraction reached about 80% at a strain of 1.8, 930 °C and 1×10^{-4} s^{-1}. The height reduction was more than 85% for compression. Meanwhile, low speed deformation should be carried out isothermally, which restrains its application. The microstructure coarsening is also significant. So, low speed deformation may not be a good method for industrial application. The strip α may also be globularized by severe plastic deformation, which is commonly used to obtain ultrafine-grained material. ZHAO et al [26] used equal channel angular pressing to refine the primary α phase of two phase titanium alloy. The initial particle size is comparable to that in this work. However, that method can only handle small billet.

Combining hot deformation with annealing, the two factors can also be fulfilled. Hot deformation is used to kink the strips and create more boundaries inside. It is better if the deformation temperature is lower and the applied strain is larger. Meanwhile, annealing aims to split the strips. A high annealing temperature is recommended as it can thin the strips by phase transformation and promote diffusion controlled splitting process. Long time annealing is unnecessary because boundary splitting takes place in the early stage of annealing. Figure 18 shows the microstructure of a specimen deformed at 600 °C and 0.1 s^{-1} to 40% reduction and then held at 970 °C for 2 h. The micrograph was taken at the center of the workpiece (the large deformation zone). The α strips were well split after hot working.

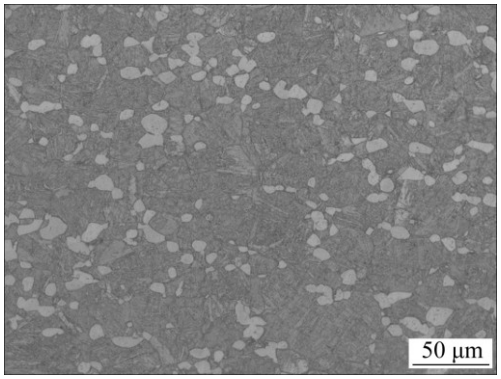

Fig. 18 Microstructure showing break-down of α strips by hot working

4 Conclusions

1) The globularization mechanisms of α strips during hot working are the same to those of lamellar structure. Due to the larger size of α strips, boundary splitting and termination migration play more important roles than coarsening.

2) The α strips can be broken down by high temperature annealing. But it is hard to obtain fully globularized structure by annealing. Stability of the α strips is attributed to the unfavorable geometrical orientation of intra-α boundaries, the large thickness of the strip as well as the geometrical stability of α particles. Annealing does not change the distribution of α particles.

3) Both predeformation and low speed deformation accelerate the globularization of α strips. The roles of deformation in morphology transformation include direct change in shape by compressing and kinking the strips, promotion of boundary splitting and termination migration by increasing high angle grain boundaries and interfacial area, promotion of coarsening by forming dislocation structures. Deformation also results in randomly distributed α particles.

4) Coarsening is significant during prolonged annealing. Low speed deformation greatly promotes grain growth. Predeformation does not affect the coarsening process.

5) Break-down of α strips may be achieved by imposing large strain in two phase region followed by annealing in near β region.

References

[1] LÜTJERING G, WILLIAMS J C. Titanium [M]. 2nd ed. Berlin: Springer-Verlag, 2007.

[2] CABIBBO M, ZHEREBTSOV S, MIRONOV S, SALISHCHEV G. Loss of coherency and interphase α/β angular deviation from the Burgers orientation relationship in a Ti−6Al−4V alloy compressed at 800 °C [J]. Journal of Materials Science, 2013, 48: 1100−1110.

[3] ZHEREBTSOV S, MURZINOVA M, SALISHCHEV G, SEMIATIN S L. Spheroidization of the lamellar microstructure in Ti−6Al−4V alloy during warm deformation and annealing [J]. Acta Materialia, 2011, 59: 4138−4150.

[4] LI L, LUO J, YAN J J, LI M Q. Dynamic globularization and restoration mechanism of Ti−5Al−2Sn−2Zr−4Mo−4Cr alloy during isothermal compression [J]. Journal of Alloys and Compounds, 2015, 622: 174−183.

[5] DONG X G, LU S Q, ZHENG H Z. Dynamic spheroidization kinetics behavior of Ti−6.5Al−2Zr−1Mo−1V alloy with lamellar microstructure [J]. Transactions of Nonferrous Metals Society of China, 2016, 26: 1301−1309.

[6] PARK C H, WON J W, PARK J W, SEMIATIN S L, CHONG S L. Mechanisms and kinetics of static spheroidization of hot-worked Ti−6Al−2Sn−4Zr−2Mo−0.1Si with a lamellar microstructure [J]. Metallurgical and Materials Transactions A, 2012, 43: 977−985.

[7] MA X, ZENG W D, TIAN F, ZHOU Y. The kinetics of dynamic globularization during hot working of a two phase titanium alloy with starting lamellar microstructure [J]. Materials Science and Engineering A, 2012, 548: 6−11.

[8] FAN X G, YANG H, YAN S L, GAO P F. Mechanism and kinetics of static globularization in TA15 titanium alloy with transformed structure [J]. Journal of Alloys and Compounds, 2012, 533: 1−8.

[9] XU J W, ZENG W D, JIA Z Q, SUN X, ZHOU J H. Static globularization kinetics for Ti-17 alloy with initial lamellar microstructure [J]. Journal of Alloys and Compounds, 2014, 603: 239−247.

[10] FAN X G, YANG H, GAO P F, YAN S L. Morphology development of the elongated α phases in hot working of large-scale titanium alloy plate [J]. Transactions of Nonferrous Metals Society of China, 2013, 23: 3508−3516.

[11] SEMIATIN S L, CORBETT M W, FAGIN P N, SALISHCHEV G A, LEE C S. Dynamic-coarsening behavior of an α/β titanium alloy [J]. Metallurgical and Materials Transactions A, 2006, 37: 1125−1136.

[12] MOTYKA M, SIENIAWSKI J, ZIAJA W. Microstructural aspects of superplasticity in Ti−6Al−4V alloy [J]. Materials Science and Engineering A, 2014, 599: 57−63.

[13] PILCHAK A L, SZCZEPANSKI C J, SHAFFER J A, SALEM A A, SEMIATIN S L. Characterization of microstructure, texture, and microtexture in near-α titanium mill products [J]. Metallurgical and Materials Transactions A, 2013, 44: 4881−4890.

[14] LI H W, JI Z, YANG H. Quantitative characterization of lamellar and equiaxed α phases of (α+β) titanium alloy using a robust approach for touching features splitting [J]. Materials Characterization, 2013, 76: 6−20.

[15] STEFANSSON N, SEMIATIN S L. Mechanisms of globularization of Ti−6Al−4V during static heat treatment [J]. Metallurgical and Materials Transactions A, 2003, 34: 691−698.

[16] TEIXEIRA J, APPOLAIRE B, AEBY-GAUTIER E, DENIS S, BRUNESEAUX F. Modeling of the effect of the β phase deformation on the α phase precipitation in near-β titanium alloys [J]. Acta Materialia, 2006, 54: 4261−4271.

[17] VO P, JAHAZI M, YUE S, BOCHER P. Flow stress prediction during hot working of near-α titanium alloys [J]. Materials Science and Engineering A, 2007, 447: 99−110.

[18] BIELER T R, SEMIATIN S L. The origins of heterogeneous deformation during primary hot working of Ti−6Al−4V [J]. International Journal of Plasticity, 2002, 18: 1165−1189.

[19] LUO J, LI L, LI M Q. Deformation behavior of Ti−5Al−2Sn−2Zr−4Mo−4Cr alloy with two initial microstructures during hot working [J]. Transactions of Nonferrous Metals Society of China, 2016, 26: 414−422.

[20] SESHACHARYULU T, MEDEIROS S C, FRAZIER W G, PRASAD Y V R K. Microstructural mechanisms during hot working of commercial grade Ti−6Al−4V with lamellar starting structure [J]. Materials Science and Engineering A, 2002, 325: 112−125.

[21] KAWASAKI M, LANGDON T G. Review: Achieving superplastic properties in ultrafine-grained materials at high temperatures [J]. Journal of Materials Science, 2016, 51: 19−32.

[22] DOHERTY R D. Diffusive phase transformations in the solid state [M]//CAHN R W, HAASEN P. Physical Metallurgy, 4th ed. Amsterdam: Elsevier, 1996: 1363−1505.

[23] WU C, YANG H, LI H W. Primary α grain coarsening behaviors of Ti−6Al−2Zr−1Mo−1V alloy in the α+β two-phase field [J]. Journal of Materials Engineering and Performance, 2013, 22: 2257−2566.

[24] SEMIATIN S L, KIRBY B C, SALISHCHEV G A. Coarsening behavior of an α−β titanium alloy [J]. Metallurgical and Materials Transactions A, 2004, 35: 2809−2819.

[25] XU J W, ZENG W D, JIA Z Q, SUN X, ZHOU J H. Microstructure coarsening behavior of Ti-17 alloy with equiaxed α during heat treatment [J]. Journal of Alloys and Compounds, 2015, 618: 343−348.

[26] ZHAO Y, GUO H Z, SHI Z F. Microstructure evolution of TA15 titanium alloy subjected to equal channel angular pressing and subsequent annealing at various temperatures [J]. Journal of Materials Processing Technology, 2011, 211: 1364−1371.

两相钛合金热加工中初生带状 α 相形态演变

樊晓光，杨 合，高鹏飞，左 瑞，雷鹏辉，吉 喆

西北工业大学 材料学院 凝固技术国家重点实验室，西安 710072

摘 要：为实现钛合金初生带状 α 相的球化，以具有这种组织的 TA15 钛合金为对象，研究其在热加工中的组织演变。结果表明：带状 α 相形态演变的机理与片层组织球化机理相同。由于带状 α 相尺寸较大，界面分离和末端物质迁移机制较粗化更为重要。带状 α 相在退火中较为稳定，主要原因是：内部晶界的几何取向不利于球化、带状组织的宽度较大和 α 粒子几何稳定性高。预变形和低速变形通过以下方式加速球化：直接改变 α 相的几何形状、通过增加大角度晶界以及相界的面积促进界面分离和末端物质迁移、通过形成位错结构促进粗化。采用大预变形结合高温退火是球化带状 α 相的有效途径。

关键词：钛合金；初生带状 α 相；球化；形态演变；热加工；粗化

(Edited by Xiang-qun LI)